Available online at www.sciencedirect.com
SCIENCE DIRECT
Geochimica et Cosmochimica Acta 70 (2006) 767–779
Geochimica
www.elsevier.com/locate/gca

Oxygen isotope compositions of chondrules in CR chondrites

Alexander N. Krot [a,*], Guy Libourel [b,c], Marc Chaussidon [b]

[a] Hawai'i Institute of Geophysics and Planetology, School of Ocean and Earth Science and Technology, University of Hawai'i at Manoa, Honolulu, HI 96822, USA
[b] Centre de Recherches Pétrographiques et Géochimiques, CNRS-UPR2300, 15, rue Notre Dame des Pauvres, BP20, 54501 Vandoeuvre-les-Nancy, France
[c] Ecole Nationale Supérieure de Géologie, INPL, Rue du Doyen Marcel Roubault, BP40, 54501 Vandoeuvre-les-Nancy, France

Received 29 November 2004; accepted in revised form 25 August 2005

Abstract

We report in situ ion microprobe analyses of oxygen isotopic compositions of olivine, low-Ca pyroxene, high-Ca pyroxene, anorthitic plagioclase, glassy mesostasis, and spinel in five aluminum-rich chondrules and nine ferromagnesian chondrules from the CR carbonaceous chondrites EET92042, GRA95229, and MAC87320. Ferromagnesian chondrules are isotopically homogeneous within ±2‰ in $\Delta^{17}O$; the interchondrule variations in $\Delta^{17}O$ range from 0 to −5‰. Small oxygen isotopic heterogeneities found in two ferromagnesian chondrules are due to the presence of relict olivine grains. In contrast, two out of five aluminum-rich chondrules are isotopically heterogeneous with $\Delta^{17}O$ values ranging from −6 to −15‰ and from −2 to −11‰, respectively. This isotopic heterogeneity is due to the presence of ^{16}O-enriched spinel and anorthite ($\Delta^{17}O = -10$ to −15‰), which are relict phases of Ca,Al-rich inclusions (CAIs) incorporated into chondrule precursors and incompletely melted during chondrule formation. These observations and the high abundance of relict CAIs in the aluminum-rich chondrules suggest a close genetic relationship between these objects: aluminum-rich chondrules formed by melting of spinel–anorthite–pyroxene CAIs mixed with ferromagnesian precursors compositionally similar to magnesium-rich (Type I) chondrules. The aluminum-rich chondrules without relict CAIs have oxygen isotopic compositions ($\Delta^{17}O = -2$ to −8‰) similar to those of ferromagnesian chondrules. In contrast to the aluminum-rich chondrules from ordinary chondrites, those from CRs plot on a three-oxygen isotope diagram along the carbonaceous chondrite anhydrous mineral line and form a continuum with amoeboid olivine aggregates and CAIs from CRs. We conclude that oxygen isotope compositions of chondrules resulted from two processes: homogenization of isotopically heterogeneous materials during chondrule melting and oxygen isotopic exchange between chondrule melt and ^{16}O-poor nebular gas.

1. Introduction

Oxygen isotopic compositions of chondritic components [Ca,Al-rich inclusions (CAIs), amoeboid olivine aggregates (AOAs), chondrules, and matrix] in combination with mineralogical observations, theoretical modeling, and oxygen isotopic diffusion and exchange experiments on the calcium–aluminum-rich and ferromagnesian silicate melts and minerals can potentially provide important constraints on the genetic relationship between the chondritic components (e.g., Clayton et al., 1977; Clayton, 1993, 2002; Ryerson and McKeegan, 1994; Yu et al., 1995; Yurimoto et al., 1989, 1994, 1998; McKeegan et al., 1998; Young and Russell, 1998; Hiyagon and Hashimoto, 1999; Scott and Krot, 2001; Yurimoto and Kuramoto, 2004; Krot et al., 2004a; Boesenberg et al., 2004; Lyons and Young, 2005). For example, most refractory inclusions in primitive chondrites are ^{16}O-enriched ($\Delta^{17}O \leqslant -20$‰; $\Delta^{17}O = \delta^{17}O - 0.52 \times \delta^{18}O$) compared to the majority of chondrules and matrices ($\Delta^{17}O \geqslant -5$‰), suggesting formation in isotopically distinct gaseous reservoirs separated in time and/or in space (McKeegan et al., 1998; Krot et al., 2002a, 2004b; Itoh and Yurimoto, 2003; Scott and Krot, 2003; Yurimoto and Kuramoto, 2004).

To understand the genetic relationship between CAIs and chondrules and evolution of the oxygen isotopic composition of the inner solar nebula, we initiated a study of

* Corresponding author. Fax: +1 808 956 6322.
E-mail address: sasha@higp.hawaii.edu (A.N. Krot).

0016-7037/$ - see front matter © 2006 Published by Elsevier Inc.
doi:10.1016/j.gca.2005.08.028

the mineralogy, petrography, oxygen, and ^{26}Al–^{26}Mg isotopic systematics of chondrules and refractory inclusions from primitive ordinary and carbonaceous chondrites. Based on the detailed mineralogical study of aluminum-rich (>10 wt% Al_2O_3) chondrules from the CV, CR, and ungrouped carbonaceous chondrites Adelaide and Acfer 094, it is inferred that aluminum-rich chondrules (ARCs) formed by melting of the spinel–anorthite–pyroxene CAIs mixed with ferromagnesian precursors compositionally similar to magnesian (Type I) chondrules (Krot and Keil, 2002; Krot et al., 2001, 2002b, 2004c). This model, however, appears to be inconsistent with oxygen isotopic compositions of ARCs from unequilibrated ordinary chondrites Sharps (H3.4), Inman (L3.4), Chainpur (LL3.4), and Quinyambie (L3.4), which on a three-oxygen isotope diagram (Fig. EA1) define a slope of about 0.8 (Russell et al., 2000), distinct from a slope of about 1 along which most CAIs plot [carbonaceous chondrite anhydrous mineral (CCAM) line]. To minimize the effects of thermal metamorphism and to test the model of Krot and Keil (2002), we measured in situ oxygen isotopic compositions of individual minerals in aluminum-rich and ferromagnesian chondrules from the Antarctic CR carbonaceous chondrites Elephant Moraine (EET) 92042, Graves Nunatak (GRA) 95229, and MacAlpine Hills (MAC) 87320. These meteorites experienced aqueous alteration to a very minor degree and show no evidence for thermal metamorphism (Krot et al., 2002c). The obtained results are compared with oxygen isotopic compositions of CAIs and AOAs from CR chondrites which have been recently reported by Aléon et al. (2002).

2. Analytical procedures

Five aluminum-rich chondrules (ARCs) rich in plagioclase and seven ferromagnesian chondrules from the Antarctic CR carbonaceous chondrites EET92042, 22, EET92174, 7 and GRA95229, 9 were studied using optical microscopy, backscattered electron (BSE) imaging, X-ray elemental mapping, electron probe microanalysis (EPMA), and ion microprobe analysis. BSE images were obtained with the JEOL JSM-5900LV scanning electron microscopes (SEM) using a 15 kV accelerating voltage and 1–2 nA beam current. Electron probe analyses were performed with a Cameca SX-50 electron microprobe using a 15 kV accelerating voltage, 10–20 nA beam current, beam size of ~1–2 μm and wavelength dispersive X-ray spectroscopy. For each element, counting times on both peak and background were 30 s (10 s for Na and K). Matrix effects were corrected using PAP procedures. The element detection limits with the Cameca SX-50 were (in wt%): 0.04 (K_2O), 0.07 (Cr_2O_3), 0.08 (Na_2O), and 0.09 (FeO). X-ray elemental maps with a resolution of 2–3 μm/pixel were acquired with five spectrometers of the Cameca microprobe operating at 15 kV accelerating voltage, 50–100 nA beam current and ~1–2 μm beam size.

Oxygen isotopic compositions of olivine, pyroxenes, spinel, anorthite, and mesostasis were measured in situ with the CRPG-CNRS Cameca IMS 1270 ion microprobe operated in multicollection mode. ^{16}O and ^{18}O were measured using Faraday cups; ^{17}O was measured using the axial electron multiplier. A Cs^+ primary beam of 10 nA was used to produce ion probe sputter pits approximately 25–30 μm in diameter. With such conditions, the count rate was $\sim 2 \times 10^6$ counts per second for ^{18}O. Corrections for instrumental mass fractionation (IMF), counting statistics, and uncertainty in standard compositions were applied. The IMF was corrected using terrestrial standards: olivine, clinopyroxene, orthopyroxene, MORB glass, adularia, spinel, and quartz. Under the analytical conditions employed, the total precision (2σ) of individual oxygen isotopic analyses is better than 1.5‰ for both $\delta^{18}O$ and $\delta^{17}O$. Oxygen isotopic compositions are reported as per mil deviations from SMOW (Standard Mean Ocean Water) ($\delta^{18}O$ and $\delta^{17}O$) and as ^{16}O excesses relative to terrestrial samples ($\Delta^{17}O$). Following oxygen isotopic measurements, each chondrule analyzed was re-examined in BSE and secondary electron images to verify the locations of the sputtered craters and mineralogy of the phases analyzed.

3. Results

The mineralogy and petrology of aluminum-rich and ferromagnesian chondrules from CR chondrites, including those studied for oxygen isotopic compositions, have been recently described by Krot and Keil (2002) and by Krot et al. (2004d). In this paper, we only summarize the major mineralogical characteristics of the chondrules analyzed. Because some of the chondrules show evidence for oxygen isotopic heterogeneity, we illustrate the positions of ion probe spots in these chondrules.

Aluminum-rich chondrules in CR chondrites have porphyritic or microporphyritic textures and are magnesium-rich: Fa and Fs contents of olivine and pyroxenes are <2–3 mol%. They typically consist of enstatite, pigeonite, and olivine phenocrysts, interstitial anorthitic plagioclase, pigeonite, and augite, Fe,Ni-metal nodules, and crystalline mesostasis composed of anorthitic plagioclase, silica, pigeonite, and augite (Figs. 1–4). Chondrules #1 from EET92042 (Fig. 3) and # 1 from EET92174 (Fig. 4) contain large regions rich in anorthite and spinel, which may represent remelted relict CAIs (Krot and Keil, 2002).

Enstatite ($Fs_{0.5-1}Wo_{1-5}$) and pigeonite ($Fa_{1-2}Wo_{5-8}$) have high concentrations of Al_2O_3 (0.5–4 wt%), TiO_2 (up to 1.2 wt%), and Cr_2O_3 (0.4–1.6 wt%) and moderate concentrations of MnO (0.1–0.6 wt%). Augite ($Fs_{1-2}Wo_{35-45}$) has higher concentrations of Al_2O_3 (1–6 wt%), TiO_2 (0.5–5.5 wt%), Cr_2O_3 (0.3–3 wt%), and MnO (up to 2.5 wt%). Olivine is Cr-rich (up to 0.9 wt% Cr_2O_3) and poor in MnO, CaO, and Al_2O_3. Plagioclase (An_{85-100}) has rather high contents of MgO (up to 1.2 wt%). Spinel grains are

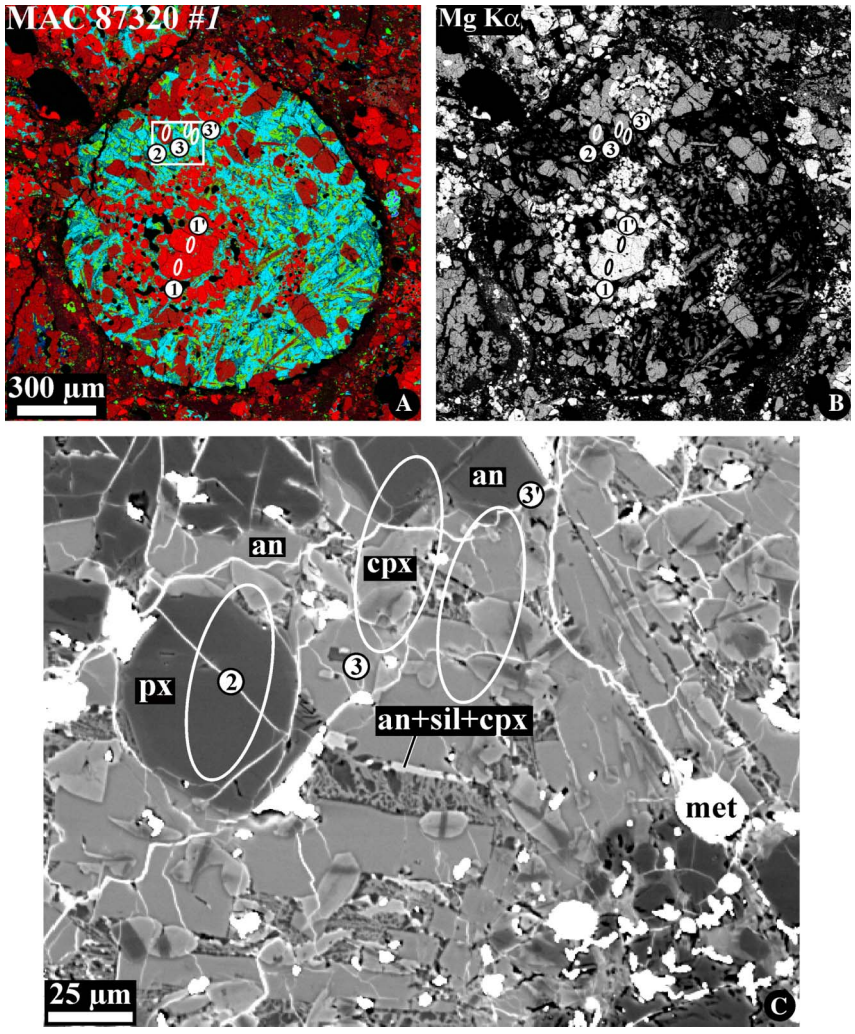

Fig. 1. Combined X-ray elemental map in Mg (red), Ca (green), and Al Kα (blue) (A), elemental map in Mg (B), and BSE image (C) of the aluminum-rich chondrule #1 from MAC87320. The region outlined in "A" is shown in detail in "C." Chondrule consists of low-Ca pyroxene (px), forsteritic olivine (ol), anorthitic plagioclase (an), high-Ca pyroxene (cpx), Fe,Ni-metal nodules (met), and crystalline mesostasis composed of anorthitic plagioclase, silica (sil), and high-Ca pyroxene. The white vein-like features in "C" are cracks filled by terrestrial weathering products; the irregularly shaped white regions in "C" are gold particles of coating used for an Al-Mg isotope study. Here and in Figs. 2–5 ion microprobe spots produced during oxygen-isotopic measurements are outlined; numbers near ellipsoids correspond to analysis numbers listed in Table 1.

FeO-poor (<1.7 wt%) and Cr-bearing (up to 8.7 wt% Cr_2O_3). Although Cr concentrations in spinel grains range broadly within a chondrule, no compositional zoning has been observed within an individual spinel grain; instead, Cr-poor spinel is overgrown by Cr-rich spinel (Fig. 3). Fe,Ni-metal nodules have kamacitic compositions and are compositionally uniform within a chondrule.

Most ferromagnesian chondrules have porphyritic textures and are composed of magnesium olivine and low-Ca pyroxene phenocrysts (Fa and Fs <2–3 mol%) and glassy or microcrystalline mesostasis (Figs. 5A–D); the only exception is a ferroan porphyritic olivine (Type II) chondrule MAC87320 #13 containing ferrous ($Fa_{30–40}$) olivine phenocrysts (Fig. 5E).

Oxygen isotopic compositions of aluminum-rich and ferromagnesian chondrules analyzed are listed in Table 1 and plotted in Figs. 6 and 7. Although some spots overlapped on several minerals or cracks (Figs. 1–3), we consider that the main contribution for the oxygen isotopic measurements come from the dominant mineral of the beam area (see Table 1), and that the contributions from the other associated minerals are negligible. On a three-oxygen isotopic diagram, both chondrule types plot along the carbonaceous chondrite anhydrous mineral (CCAM) line (Fig. 8A). Olivine, pyroxene, and mesostasis in individual ferromagnesian chondrules are isotopically uniform; the only exceptions are chondrules #10 and #11 from MAC87320 (Figs. 5C and D), in which the largest olivine grains are slightly ^{16}O-enriched relative to the finer-grained olivine and pyroxene phenocrysts (Table 1; Figs. 6A, B and 8A, B). The interchondrule variations are small: $\Delta^{17}O$ ranges from 0 to −5‰. The ferrous olivine chondrule #13 from MAC87320 (Fig. 5E) has the heaviest oxygen isotopic composition (Table 1; Figs. 6C and 8A, B).

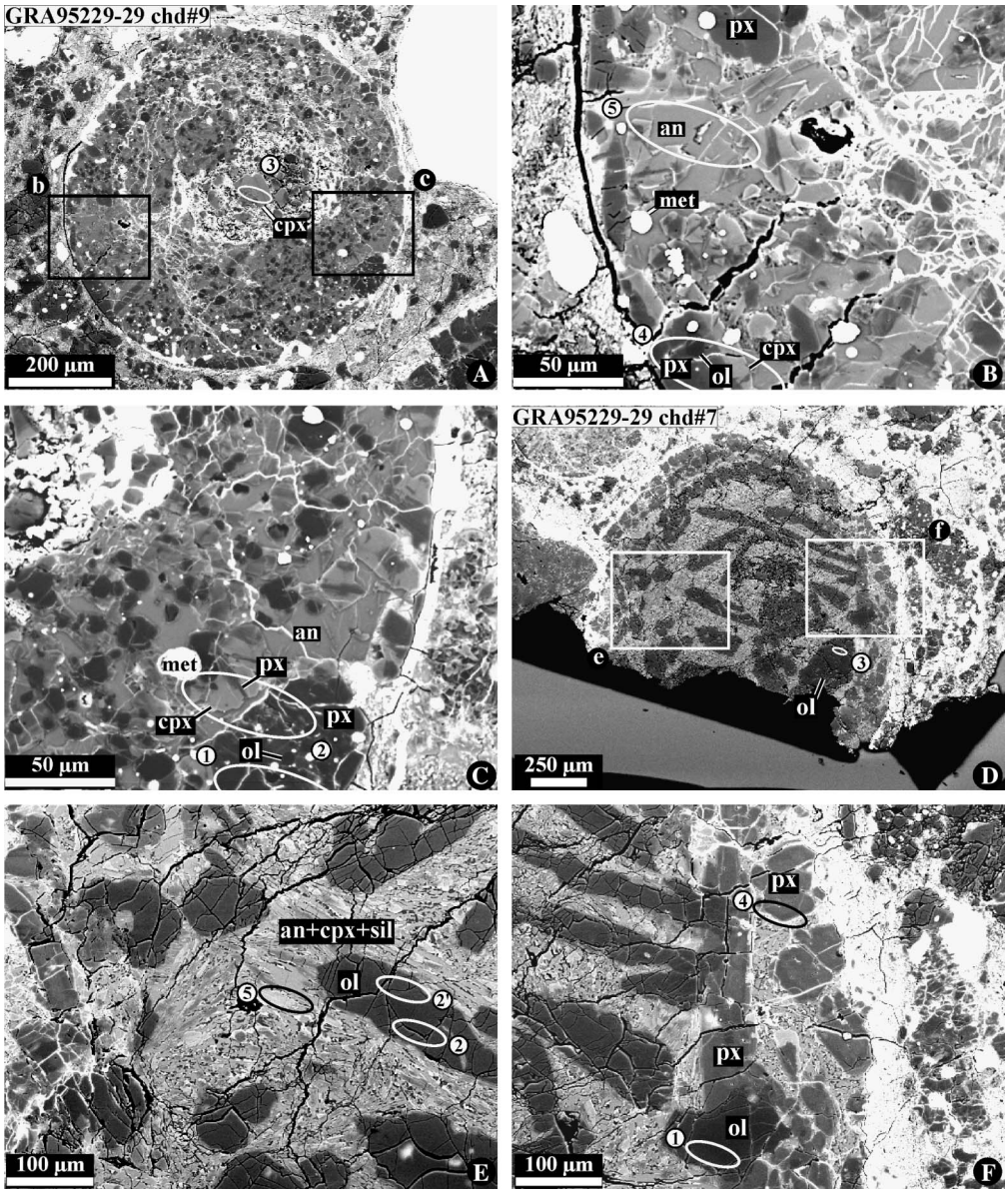

Fig. 2. BSE images of the aluminum-rich chondrules #9 (A–C) and #7 (D–F) from GRA95229. Regions outlined in "A" and "D" are shown in detail in "B, C" and "E, F," respectively. Chondrule #7 has a microporphyritic texture and consists of forsteritic olivine, low-Ca pyroxene, high-Ca pyroxene, lath-shaped anorthitic plagioclase, silica-plagioclase mesostasis, and Fe,Ni-metal nodules. Chondrule #9 has a porphyritic texture and consists of forsteritic olivine, low-Ca pyroxene, and crystalline mesostasis composed of silica, plagioclase, and high-Ca pyroxene.

The aluminum-rich chondrules containing CAI-like regions, #1 from EET92042 (Fig. 3) and #1 from EET92174 (Fig. 4), have heterogeneous oxygen isotopic compositions with $\Delta^{17}O$ varying from −15 to −6‰ and from −11 to −2‰, respectively (Table 1; Figs. 7A and B). This isotopic heterogeneity is due to the presence of ^{16}O-enriched spinel and anorthite, which have been interpreted to represent relict CAIs incompletely destroyed during chondrule melting (Krot and Keil, 2002). The aluminum-rich chondrules without relict CAIs have oxygen isotopic compositions similar to those of ferromagnesian chondrules (Table 1; Figs. 6 and 7C–E).

4. Discussion

4.1. Evidence for the presence of ^{16}O-rich CAIs among aluminum-rich chondrule precursors

It has been recently concluded that refractory inclusions originated in an ^{16}O-rich gaseous reservoir, whereas chondrules formed in the presence of a ^{16}O-poor nebular gas (e.g., Scott and Krot, 2001; Krot et al., 2002a, 2004a; Clayton, 2002; Itoh and Yurimoto, 2003; Yurimoto and Kuramoto, 2004). Based on the mineralogical and petrographic observations, Krot and co-authors (Krot and Keil, 2002; Krot et al., 2001, 2002b, 2004c) inferred that ARCs

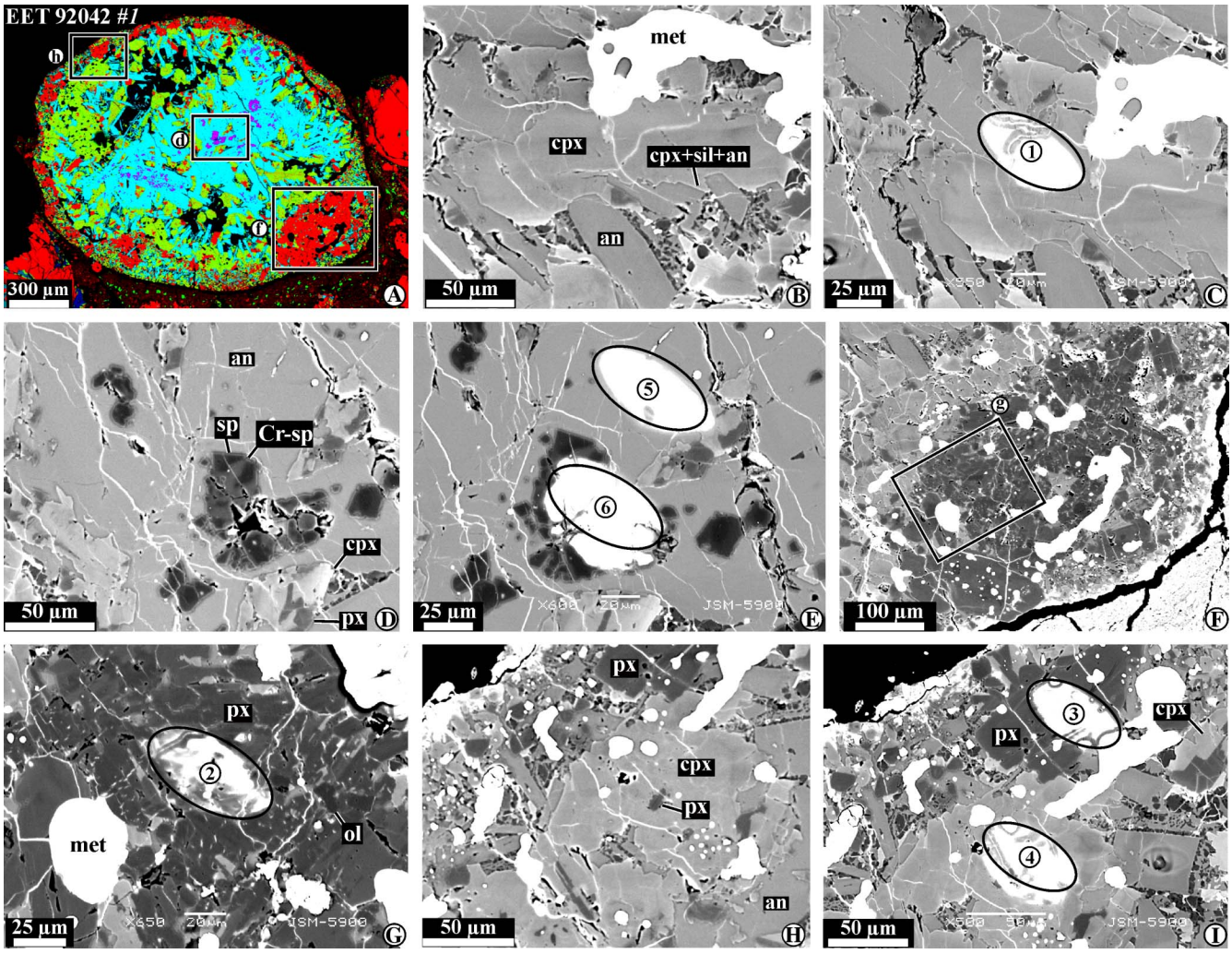

Fig. 3. Combined X-ray elemental map in Mg (red), Ca (green), and Al Kα (blue) (A) and BSE images (B–I) of the aluminum-rich chondrule #1 from EET92042. Regions outlined in "A" are shown in detail in "D, E," "F, G," and "H, I"; region outlined in "F" is shown in detail in "G." The chondrule consists of anorthitic plagioclase poikilitically enclosing Cr-rich (Cr-sp) and Cr-poor (sp) spinel grains, high-Ca pyroxene, low-Ca pyroxene, Fe,Ni-metal nodules, minor forsteritic olivine, and crystalline mesostasis composed of silica, anorthitic plagioclase, and high-Ca pyroxene. Images "B" and "C," "D" and "E," "F" and "G," and "H" and "I" show the same regions before and after ion probe analyses.

formed by melting to various degrees of the spinel–anorthite–pyroxene CAIs mixed with ferromagnesian precursors compositionally similar to Type I chondrules. A similar conclusion had been previously reached by other researchers as well (e.g., Kring and Holmen, 1988; Kring and Boynton, 1990; Sheng et al., 1991; Jones and Brearley, 1994; Maruyama et al., 1999; Maruyama and Yurimoto, 2003). The oxygen isotopic compositions of the ARCs from CR chondrules, support this model: the ^{16}O-rich isotopic signature in the ARCs is observed only in phases interpreted as relict CAI minerals incompletely melted during chondrule formation (Krot and Keil, 2002).

4.2. Evidence for oxygen isotopic exchange between chondrule melts and the solar nebular gas

Although ferromagnesian chondrules are much more abundant than aluminum-rich chondrules in all chondrite groups, a systematic search for the refractory inclusion-bearing chondrules using high resolution X-ray elemental mapping and BSE imaging revealed that relict refractory inclusions are exceptionally rare in ferromagnesian chondrules (Bishoff and Keil, 1984; Itoh et al., 2002; Yurimoto and Wasson, 2002; Krot and Keil, 2002; Krot et al., 1999, 2001, 2002b, 2004c). In contrast, more than 15% of aluminum-rich chondrules from Acfer 094, Adelaide, CV, and CR carbonaceous chondrites contain relict CAIs and AOAs, indicating a close genetic relationship between the aluminum-rich chondrules and refractory inclusions (Krot and Keil, 2002; Krot et al., 2001, 2002b, 2004c,e). Based on these observations, we infer that the vast majority of aluminum-rich chondrules in carbonaceous chondrites formed by melting of CAI-like precursors mixed with ferromagnesian chondrule precursors.

Based on petrographic observations, the ARCs can be divided into two groups: with and without relict CAIs;

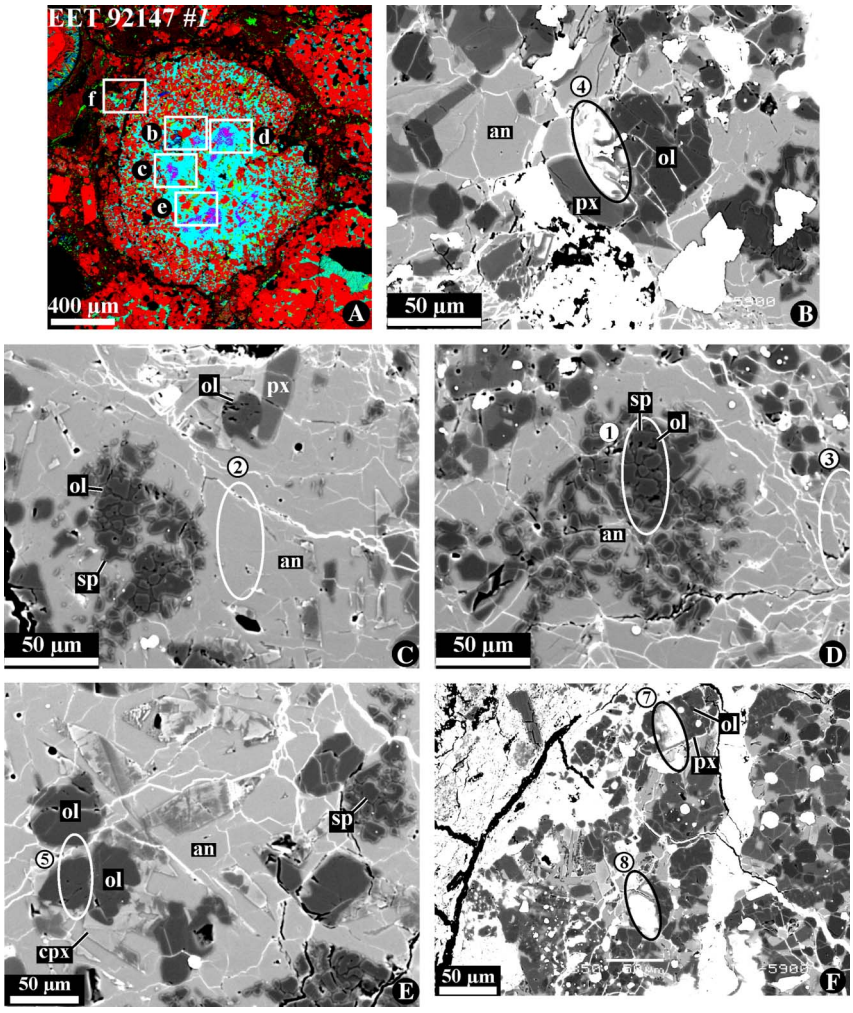

Fig. 4. Combined X-ray elemental map in Mg (red), Ca (green), and Al Kα (blue) (A) and BSE images (B–F) of the aluminum-rich porphyritic olivine–pyroxene chondrule #1 from EET92147. Regions outlined in "A" are shown in detail in "E–F." The chondrule consists of high-Ca pyroxene, low-Ca pyroxene, forsteritic olivine, lath-shaped anorthite, silica-bearing mesostasis, and abundant Fe,Ni-metal nodules. The central part of the chondrule contains a region enriched in anorthitic plagioclase and spinel, which represents an incompletely melted CAI.

the latter appear to have been more extensively melted than the former. We suggest that the relict CAI material may have been originally present in precursors of all/most ARCs from CR chondrites, but have been subsequently dissolved in many of the host chondrule melts. Oxygen isotopic compositions of minerals in the extensively melted (relict mineral-free) aluminum-rich and ferromagnesian chondrules from CR chondrites could have resulted from (i) homogenization of oxygen isotopic compositions of initially heterogeneous precursors during melting and/or (ii) oxygen isotopic exchange between chondrule melt and the surrounding gas.

Oxygen isotopic compositions of olivines from CR chondrules measured by Leshin et al. (1998) showed that there is no significant evidence for isotopic heterogeneity among different grains in a single chondrule with the exception of a relict forsteritic grain within a Renazzo Type II chondrule, which is ^{16}O-enriched by several per mil relative to the other olivines in the chondrule. This homogeneity among the melt-grown olivines was interpreted as an evidence against oxygen isotopic exchange with nebular gas during chondrule crystallization (Leshin et al., 1998, 2000). We note that extensive oxygen isotopic exchange between chondrule-like melts and gas is observed to occur in experiments (e.g., Yu et al., 1995; Boesenberg et al., 2004).

Using the same data, Varley et al. (2002) searched for a correlation between oxygen isotopic compositions of chondrule olivines with a host chondrule convolution index (ratio of chondrule's perimeter to the perimeter of a circle with the same area as the chondrule). They found that the more ^{16}O-rich chondrules generally have the larger convolution index, possibly indicating greater gas-melt exchange for the most molten chondrules.

Because the ARCs without relict CAIs and the ferromagnesian chondrules studied have rather similar oxygen isotopic compositions and are isotopically rather uniform (Figs. 6C–F and 7C–E), we infer that the, aluminum-rich and ferromagnesian chondrules were melted

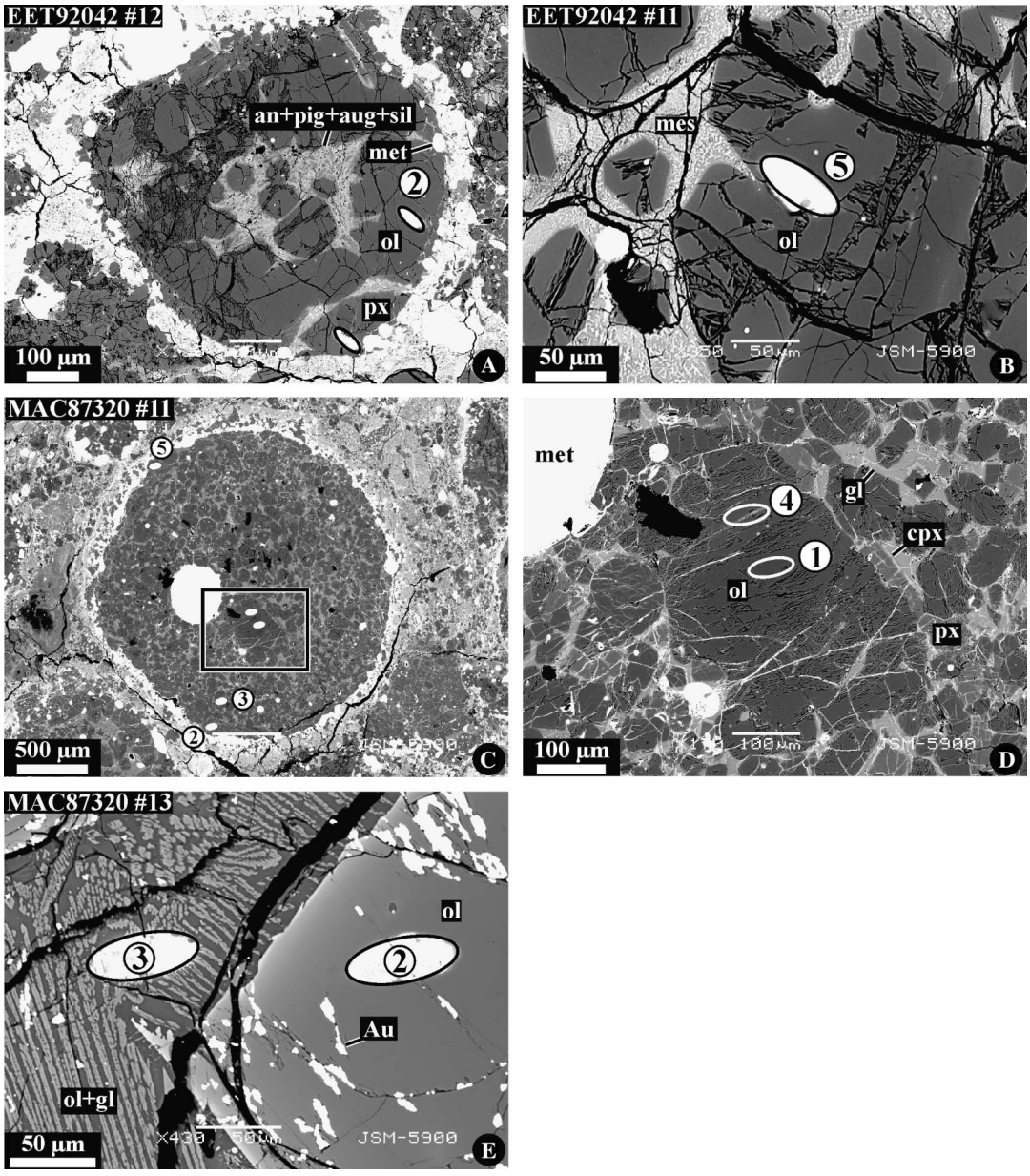

Fig. 5. BSE images of ferromagnesian chondrules studied for oxygen isotopic compositions in CR chondrites. The region outlined in "C" is shown in detail in "D." (A) Magnesian porphyritic olivine–pyroxene chondrule #12 from EET92042 consists of olivine and low-Ca pyroxene phenocrysts, and fine-grained mesostasis composed of anorthitic plagioclase, pigeonite (pig), augite (aug), and silica. (B) Magnesian porphyritic olivine–pyroxene chondrule #11 from EET92042 consists of olivine and low-Ca pyroxene phenocrysts, and mesostasis composed of high-Ca pyroxene and glass. (C, D) Magnesian porphyritic olivine–pyroxene chondrule #11 from MAC87320 consists of forsteritic olivine, low-Ca pyroxene overgrown by high-Ca pyroxene, Fe,Ni-metal nodules and glassy mesostasis. (E) Ferroan porphyritic olivine chondrule #13 from MAC87320 consists of fayalitic olivine phenocrysts and mesostasis composed of skeletal olivine crystals and glass.

and experienced oxygen isotopic exchange in a similarly ^{16}O-depleted gaseous reservoir. At the same time, the aluminum-rich chondrule #1 from EET92147 (Fig. 4), with a high proportion of unmelted CAI material, contains chondrule phenocrysts enriched in ^{16}O compared to the other ARCs (Fig. 7A). These observations may indicate that this chondrule experienced smaller degree of oxygen isotopic exchanges with the surrounding gas and its oxygen isotopic composition was largely established by melting of isotopically heterogeneous precursors.

It has been recently shown (Aléon et al., 2002) that AOAs and most CAIs from CR chondrites are ^{16}O-rich (Δ^{17}O of hibonite, melilite, spinel, pyroxene, anorthite, and forsterite $<-20‰$) and isotopically homogeneous within 3–4‰ (Figs. 8C and D), suggesting that these objects (or their precursors) formed in an ^{16}O-rich gaseous reservoir. Clearly igneous CAIs (compact Type A, Type B, and Type C) are systematically ^{16}O-depleted compared to AOAs which appear to have escaped substantial melting (Krot et al., 2004d). Among these, three compact Type A

Table 1
Ion microprobe analyses of oxygen-isotopic compositions of Al-rich and ferromagnesian chondrules in CR carbonaceous chondrites

Chondrite chd#	Type	Spot#	Min. analyzed	$\delta^{18}O$ (‰)	2σ (‰)	$\delta^{17}O$ (‰)	2σ (‰)	$\Delta^{17}O$ (‰)	2σ (‰)
EET92147 #1	ARC	2	an	−11.9	0.9	−15.6	0.6	−9.4	1.1
EET92147 #1	ARC	2′	an	−11.2	0.9	−14.2	0.4	−8.4	1.0
EET92147 #1	ARC	3	an [ol]	−9.1	0.8	−13.7	0.3	−9.0	0.9
EET92147 #1	ARC	5	ol [an]	−13.6	1.0	−16.3	0.5	−9.2	1.1
EET92147 #1	ARC	5′	ol [an]	−13.7	1.0	−16.0	0.5	−8.8	1.1
EET92147 #1	ARC	4	ol [opx+an]	−11.6	1.0	−13.7	0.5	−7.7	1.1
EET92147 #1	ARC	6	opx	−7.8	1.3	−11.9	0.8	−7.9	1.5
EET92147 #1	ARC	7	opx [ol+an]	−8.0	1.3	−11.6	0.8	−7.5	1.5
EET92147 #1	ARC	8	opx [ol+an]	−8.2	1.3	−10.4	0.7	−6.1	1.5
EET92147 #1	ARC	1	sp [an+ol]	−24.8	0.9	−28.0	0.4	−15.1	1.0
EET92042 #1	ARC	5	an	−4.1	0.8	−8.6	0.4	−6.5	0.9
EET92042 #1	ARC	4	cpx	1.4	2.4	−1.6	1.2	−2.4	2.7
EET92042 #1	ARC	1	cpx [an]	2.1	2.3	−2.0	1.2	−3.1	2.6
EET92042 #1	ARC	3	opx	−0.1	1.3	−4.3	0.7	−4.2	1.5
EET92042 #1	ARC	2	opx [ol]	0.1	1.3	−2.1	0.7	−2.2	1.4
EET92042 #1	ARC	6	sp [an]	−12.3	0.7	−16.2	0.5	−9.8	0.8
EET92042 #1	ARC	6′	sp [an]	−13.7	0.9	−17.7	0.5	−10.6	1.0
GRA95229 #7	ARC	1	ol	1.5	1.1	−3.5	0.5	−4.3	1.2
GRA95229 #7	ARC	2	ol	2.3	1.0	−1.5	0.5	−2.7	1.1
GRA95229 #7	ARC	2′	ol	1.0	0.9	−4.2	0.6	−4.7	1.0
GRA95229 #7	ARC	3	ol	1.6	1.0	−4.1	0.6	−5.0	1.2
GRA95229 #7	ARC	4	opx [an+sil+cpx]	2.1	1.4	−0.7	0.7	−1.8	1.6
GRA95229 #7	ARC	5	an+cpx [sil]	3.7	0.9	−1.3	0.4	−3.2	1.0
GRA95229 #9	ARC	5	an [cpx]	3.5	0.8	−2.2	0.5	−4.0	1.0
GRA95229 #9	ARC	3	cpx	−2.0	1.3	−5.1	0.7	−4.0	1.4
GRA95229 #9	ARC	1	opx [ol]	1.7	1.3	−1.8	0.7	−2.7	1.4
GRA95229 #9	ARC	2	opx [cpx+an]	0.2	1.3	−3.0	0.7	−3.1	1.4
GRA95229 #9	ARC	4	opx [cpx+ol+an]	0.9	1.3	−2.6	0.7	−3.0	1.5
MAC87320 #1	ARC	1	ol	−4.8	1.0	−7.5	0.5	−5.0	1.1
MAC87320 #1	ARC	1′	ol	−3.6	1.0	−7.9	0.6	−6.1	1.2
MAC87320 #1	ARC	2	opx [cpx]	−1.8	1.3	−5.9	0.7	−5.0	1.5
MAC87320 #1	ARC	3	cpx+opx [an]	0.6	0.8	−6.9	0.4	−7.2	0.9
MAC87320 #1	ARC	3′	an+cpx [opx]	−1.7	0.8	−5.5	0.4	−4.6	0.9
EET92042 #11	Type I	1	mes	−0.1	2.6	−2.7	1.3	−2.7	2.9
EET92042 #11	Type I	2	ol	−2.4	0.9	−3.6	0.5	−2.4	1.1
EET92042 #11	Type I	5	ol	0.8	1.1	−2.5	0.5	−2.9	1.2
EET92042 #11	Type I	3	opx	−3.5	1.4	−3.3	0.7	−1.5	1.6
EET92042 #11	Type I	4	opx	0.4	1.3	−2.5	0.7	−2.7	1.4
EET92042 #12	Type I	1	ol	2.4	1.1	−0.7	0.5	−1.9	1.2
EET92042 #12	Type I	2	opx [ol]	2.0	1.3	−1.0	0.7	−2.0	1.5
GRA95229 #20	Type I	1	opx	3.5	1.3	−1.7	0.7	−3.6	1.5
GRA95229 #20	Type I	2	opx	2.1	1.3	−1.0	0.6	−2.1	1.4
GRA95229 #20	Type I	3	opx	3.0	1.3	−0.7	0.7	−2.3	1.5
MAC87320 #10	Type I	1	ol	1.1	1.0	−0.8	0.5	−1.4	1.1
MAC87320 #10	Type I	3	ol	2.9	1.0	−2.9	0.6	−4.4	1.2
MAC87320 #10	Type I	3′	ol	2.7	1.4	−2.1	0.7	−3.5	1.5
MAC87320 #10	Type I	2	opx	2.1	1.4	−0.7	0.7	−1.9	1.6
MAC87320 #10	Type I	4	opx	1.7	1.3	0.7	0.7	−0.2	1.5
MAC87320 #11	Type I	1	ol	−4.9	1.0	−7.7	0.5	−5.1	1.1
MAC87320 #10	Type I	3	ol	1.5	0.9	−5.4	0.7	−6.1	1.2
MAC87320 #10	Type I	3′	ol	1.4	1.0	−4.4	0.6	−5.1	1.1
MAC87320 #10	Type I	4	ol	−5.3	1.0	−11.2	0.6	−8.5	1.2
MAC87320 #10	Type I	2	opx	1.8	1.2	−2.3	0.7	−3.3	1.4
MAC87320 #10	Type I	5	opx [ol]	1.7	1.3	−1.5	0.6	−2.4	1.4
MAC87320 #12	Type I	3	mes	3.4	2.6	−0.1	1.3	−1.9	2.9
MAC87320 #12	Type I	2	ol	2.4	1.1	−0.3	0.5	−1.5	1.2
MAC87320 #12	Type I	1	opx	3.2	1.3	0.3	0.7	−1.3	1.5

Table 1 (*continued*)

Chondrite chd#	Type	Spot#	Min. analyzed	$\delta^{18}O$ (‰)	2σ (‰)	$\delta^{17}O$ (‰)	2σ (‰)	$\Delta^{17}O$ (‰)	2σ (‰)
MAC87320 #13	Type II	3	mes	9.4	2.5	4.4	1.3	−0.5	2.8
MAC87320 #13	Type II	1	ol	8.7	0.9	3.5	0.5	−1.0	1.0
MAC87320 #13	Type II	2	ol	8.9	0.9	3.9	0.5	−0.7	1.0

ARC, aluminum-rich chondrule; an, anorthitic plagioclase; cpx, high-Ca pyroxene; mes, mesostasis; ol, olivine; opx, low-Ca pyroxene; sp, spinel. mineral listed in brackets represents a minor phase in an anlayzed spot.

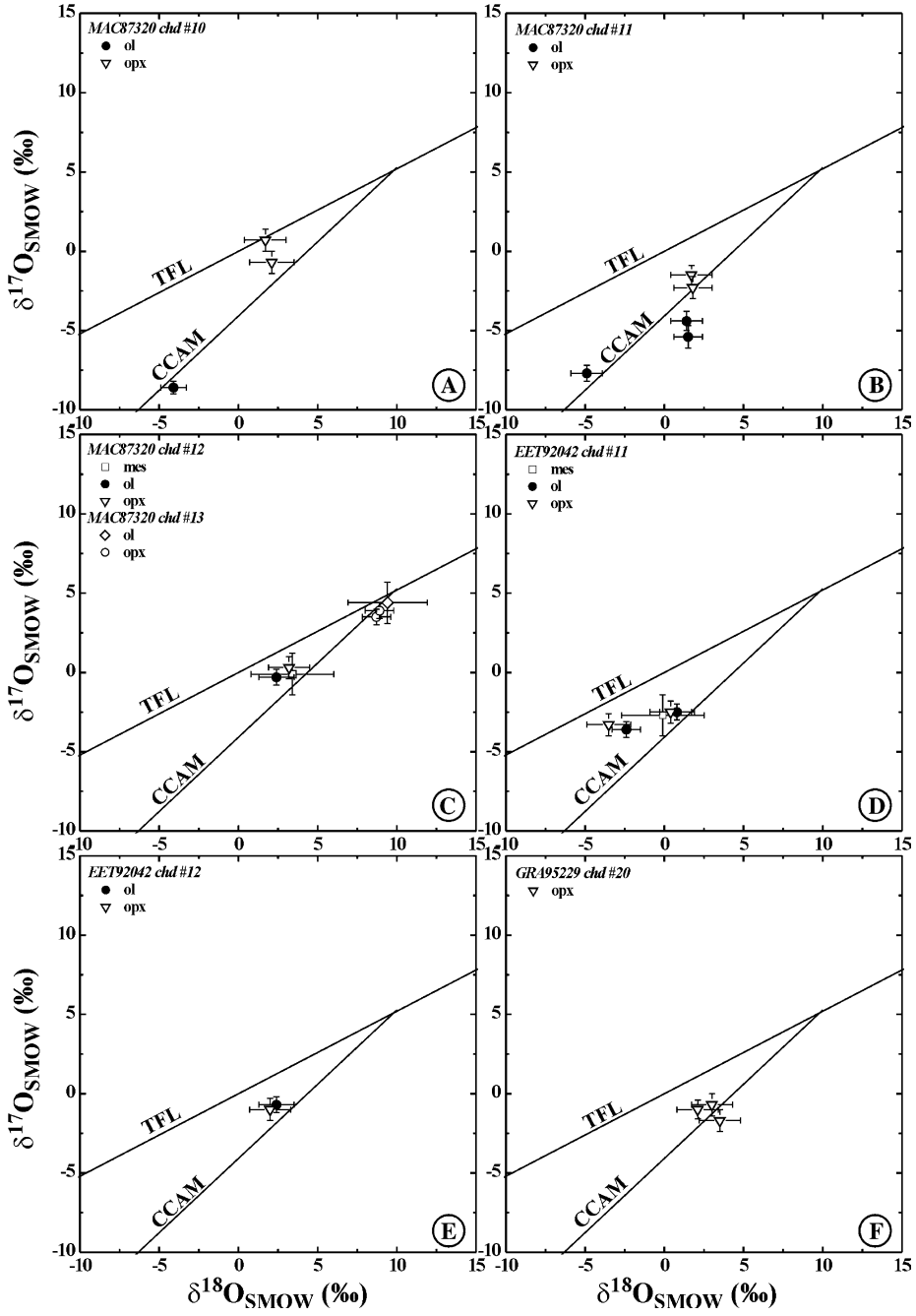

Fig. 6. Oxygen isotopic composition of ferromagnesian chondrules in CR chondrites. Most chondrules are isotopically uniform. Oxygen isotopic heterogeneity in chondrules #10 and #11 from MAC87320 is due to the presence of relict olivine grains. CCAM, carbonaceous chondrite anhydrous mixing line. Terrestrial fractionation and CCAM lines are shown for reference.

CAIs and a Type B inclusion are only slightly ^{16}O-depleted ($\Delta^{17}O \sim -18$ to -15‰; Figs. 8C and D), suggesting they experienced melting in a slightly ^{16}O-depleted gaseous reservoir. In contrast, three Type C CAIs are ^{16}O-depleted to a level observed in the CR chondrules ($\Delta^{17}O = -3$ to -18‰; Figs. 8C and D). We infer that these CAIs

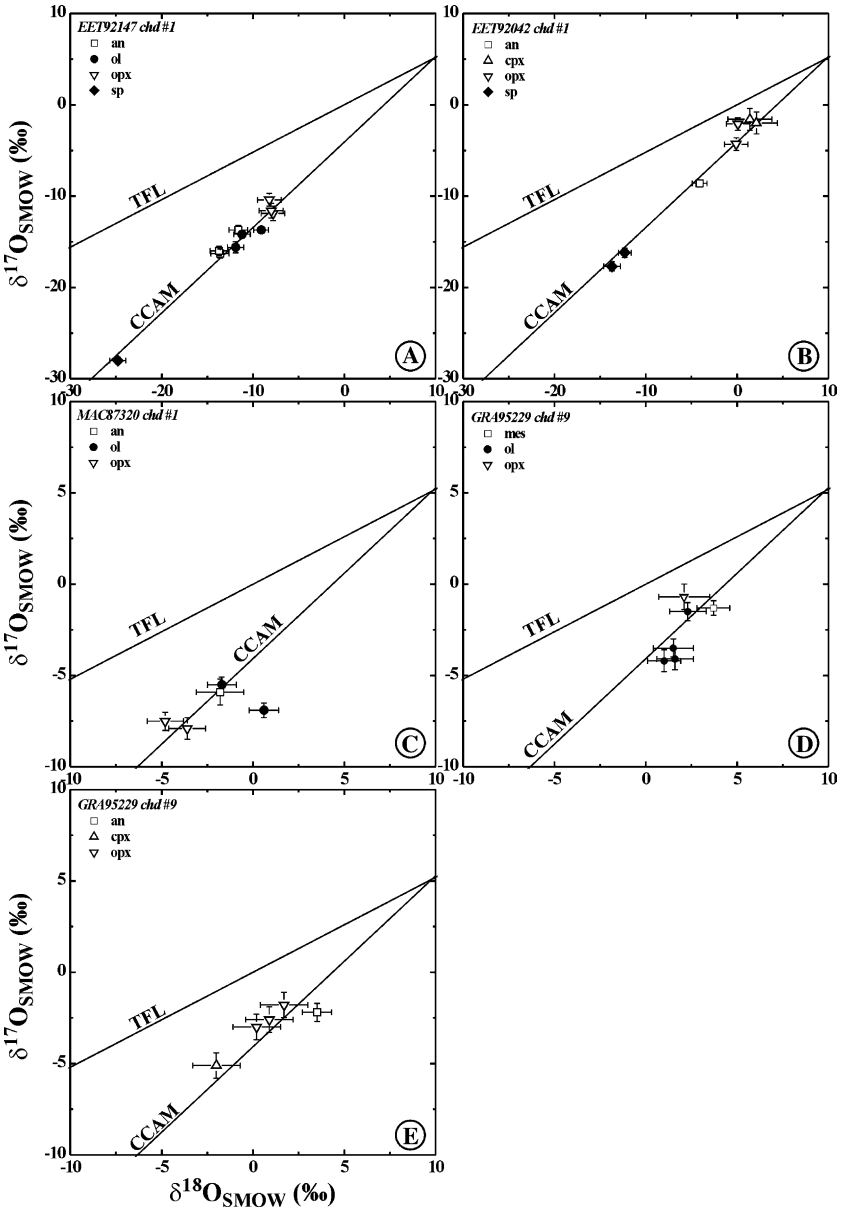

Fig. 7. Oxygen isotopic composition of aluminum-rich chondrules from CR chondrites. The oxygen isotopic heterogeneity in chondrules EET92147 #1 and EET92042 #1 is due to the presence of relict CAIs; other chondrules are isotopically uniform.

experienced melting and oxygen isotopic exchange in an ^{16}O-poor gaseous reservoir, possibly contemporaneously with chondrules (Krot et al., 2004a). The overall data for the CR AOAs, CAIs, ARCs, and ferromagnesian chondrules demonstrate that there is a continuum in oxygen isotopic compositions between these components (Fig. 8), possibly indicating an increasing degree of interaction and isotope exchange with the ^{16}O-poor gas during melting. At the same time, because AOAs and CAIs, which appear to have escaped melting (labeled as "non-igneous(?)" in Fig. 8), are similarly ^{16}O-rich, we infer that these refractory inclusions were not affected by oxygen isotopic exchange during chondrule formation. They were either absent from the chondrule-forming region at the time of chondrule formation, or, which is more likely, chondrule-forming events were rather localized and these objects escaped melting (Russell et al., 2005). The latter is consistent with the presence of relict CAIs and AOAs in chondrules (e.g., Yurimoto and Wasson, 2002; Krot et al., 2005a; Russell et al., 2005) and mineralogical and isotopic evidence for melting of some CAIs in the chondrule-forming region (Krot et al., 2005b). Since oxygen isotope exchange between gas and solid refractory inclusions is much slower than between gas and melt (Yurimoto et al., 1989, 1998; Ryerson and McKeegan, 1994), no significant oxygen isotope heterogeneity is expected to be present in the unmelted refractory inclusions.

Recently, Jones et al. (2004) described several microporphyritic Type I chondrules from Mokoia and Allende showing very large variations in oxygen isotopic compositions (Δ^{17}O from -25 to -5‰) between individual olivine grains. These chondrules may reflect incorporation of relict

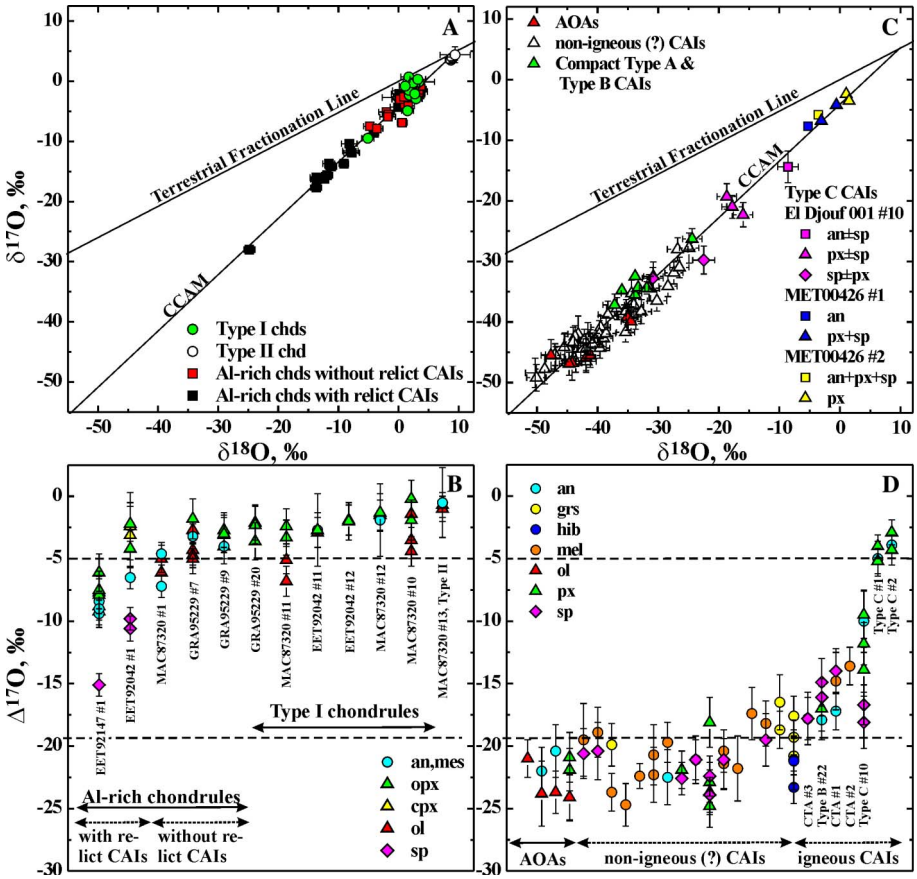

Fig. 8. Oxygen isotopic compositions of chondrules (this study) and refractory inclusions (Aléon et al., 2002) in CR carbonaceous chondrites. (A, C) $\delta^{17}O$ vs. $\delta^{18}O$; error bars are 2σ. Aluminum-rich chondrules and ferromagnesian (Type I and Type II) chondrules are ^{16}O-depleted relative to AOAs and most CAIs. Aluminum-rich chondrules with relict CAIs are ^{16}O-enriched compared to those without relict CAIs and ferromagnesian chondrules. Clearly igneous CAIs [compact Type A (CTA), Type B, and Type C] are ^{16}O-depleted compared to AOAs. The Type C CAIs are ^{16}O-depleted to a level observed in the CR chondrules. Terrestrial fractionation line and carbonaceous chondrite anhydrous mineral (CCAM) line are shown for reference. (B, D) $\Delta^{17}O$ of individual minerals in chondrules, CAIs, and AOAs; error bars are 2σ. Aluminum-rich chondrules with relict CAIs show O-isotopic heterogeneity with spinel being ^{16}O-enriched relative to anorthitic plagioclase and chondrule phenocrysts. Aluminum-rich chondrules without relict grains and ferromagnesian chondrules are isotopically uniform. The only exceptions are Type I chondrules MAC87320 #10 and MAC87320 #11 that contain ^{16}O-enriched relict olivine grains. an, anorthite; cpx, high-Ca pyroxene; grs, grossite; hib, hibonite; mel, melilite; mes, anorthitic plagioclase or mesostasis; ol, forsteritic olivine; opx, low-Ca pyroxene; px, aluminum–titanium–diopside; sp, spinel. CTA #1, GRA95229 #1; CTA #2, GRA95229 #2; CTA #3, GRA95229 #3; Type B #22, GRA95229 #22; Type C #1, MET00426 #1; Type C #2, MET00426 #2; Type C #10, El Djouf 001 #10.

grains from AOAs or incomplete oxygen isotope exchange between an early generation of ^{16}O-rich chondrules and ^{16}O-poor gas during multistage chondrule formation. Alternatively, these objects are AOAs which experienced early melting in an ^{16}O-rich gas (CAI-forming region) and subsequent incomplete melting in an ^{16}O-poor gas (chondrule-forming region).

We conclude that oxygen isotopic compositions of Al-rich chondrules from CR chondrites resulted from melting and homogenization of isotopically heterogeneous materials and from oxygen isotopic exchange between chondrule melt and nebular gas.

Acknowledgments

We thank the Antarctic Meteorite Working Group for the loan of thin sections of CR chondrites. We thank K.D. McKeegan, H. Yurimoto, and S.S. Russell for their reviews and numerous suggestions that helped to improve the paper. We thank S.S. Russell for handing the manuscript. This work was supported by NASA Grants NAGW5-10610 (A.N. Krot, P.I.), NAG5-11591 (K. Keil, P.I.), and by the French PNP program from CNRS (G. Libourel). This is Hawai'i Institute of Geophysics and Planetology publication No. 1423 and School of Ocean and Earth Science and Technology publication No. 6709.

Associate editor: Sara S. Russell

Appendix A. Supplementary data

Supplementary data associated with this article can be found, in the online version, at doi:10.1016/j.gca.2005.08.028.

References

Aléon, J., Krot, A.N., McKeegan, K.D., 2002. Ca–Al-rich inclusions and amoeboid olivine aggregates from the CR carbonaceous chondrites. *Meteorit. Planet. Sci.* **37**, 1729–1755.

Bishoff, A., Keil, K., 1984. Al-rich objects in ordinary chondrites: related origin of carbonaceous and ordinary chondrites and their constituents. *Geochim. Cosmochim. Acta* **48**, 693–709.

Boesenberg, J.S., Hewins, R.H., Chaussidon, M., 2004. Oxygen isotopic diffusion and exchange experiments on olivine and chondrule melts: preliminary results (abstract). In: *Workshop "Chondrites and the Protoplanetary Disk"*, Kauai, November 8–11, 2004, p. 9047.

Clayton, R.N., Onuma, N., Grossman, L., Mayeda, T.K., 1977. Distribution of the presolar component in Allende and other carbonaceous chondrites. *Earth Planet. Sci. Lett.* **34**, 209–224.

Clayton, R.N., 1993. Oxygen isotopes in meteorites. *Ann. Rev. Earth Planet. Sci.* **21**, 115–149.

Clayton, R.N., 2002. Self-shielding in the solar nebula. *Nature* **415**, 860–861.

Hiyagon, H., Hashimoto, A., 1999. ^{16}O excesses in olivine inclusions in Yamato-86009 and Murchison chondrites and their relation to CAIs. *Science* **283**, 828–831.

Itoh, S., Rubin, A.E., Kojima, H., Wasson, J.T., Yurimoto, H., 2002 Amoeboid olivine aggregates and AOA-bearing chondrule from Y-81020 CO3.0 chondrite: distributions of oxygen and magnesium isotopes (abstract). *Lunar Planet. Sci.* **35**, p. 1490.

Itoh, S., Yurimoto, H., 2003. Contemporaneous formation of chondrules and refractory inclusions in the early solar system. *Nature* **423**, 728–731.

Jones, R.H., Brearley, A., 1994. Reduced, plagioclase-rich chondrules in the Lance and Kainsaz CO3 chondrites (abstract). *Lunar Planet. Sci.* **25**, 641–642.

Jones, R.H., Leshin, L.A., Yunbin, G., Sharp, Z., Durakiewicz, T., Schilk, A.J., 2004. Oxygen isotope heterogeneity in chondrules from the Mokoia CV3 carbonaceous chondrites. *Geochim. Cosmochim. Acta* **68**, 3423–3438.

Kring, D.A., Holmen, B.A., 1988. Petrology of anorthite-rich chondrules in CV3 and CO3 chondrites (abstract). *Meteoritics* **23**, 282.

Kring, D.A., Boynton, W.V., 1990. Trace-element compositions of Ca-rich chondrules from Allende: relationships between refractory inclusions and ferromagnesian chondrules (abstract). *Meteoritics* **25**, 377.

Krot, A.N., Sahijpal, S., McKeegan, K.D., Weber, D., Greshake, A., Ulyanov, A.A., Hutcheon, I.D., Keil, K., 1999. Mineralogy, aluminum-magnesium and oxygen isotope studies of the relic calcium–aluminum-rich inclusions in chondrules (abstract). *Meteorit. Planet. Sci.* **34**, A68–A69.

Krot, A.N., Hutcheon, I.D., Huss, G.R., 2001. Aluminum-rich chondrules and associated refractory inclusions in the unique carbonaceous chondrite Adelaide (abstract). *Meteorit. Planet. Sci.* **36**, A105–A106.

Krot, A.N., Keil, K., 2002. Anorthite-rich chondrules in CR and CH carbonaceous chondrites: genetic link between calcium–aluminum-rich inclusions and ferromagnesian chondrules. *Meteorit. Planet. Sci.* **37**, 91–111.

Krot, A.N., McKeegan, K.D., Leshin, L.A., MacPherson, G.J., Scott, E.R.D., 2002a. Existence of an ^{16}O-rich gaseous reservoir in the solar nebula. *Science* **295**, 1051–1054.

Krot, A.N., Hutcheon, I.D., Keil, K., 2002b. Anorthite-rich chondrules in the reduced CV chondrites: evidence for complex formation history and genetic links between CAIs and ferromagnesian chondrules. *Meteorit. Planet. Sci.* **37**, 155–182.

Krot, A.N., Meibom, A., Weisberg, M.K., Keil, K., 2002c. The CR chondrite clan: implications for early solar system processes. *Meteorit. Planet. Sci.* **37**, 1451–1490.

Krot, A.N., Yurimoto, H., Hutcheon, I.D., Scott, E.R.D., 2004a. Oxygen isotope exchange in CAIs and chondrules: implication for oxygen isotope reservoirs in the solar nebula (abstract). *Meteorit. Planet. Sci.* **39**, A56.

Krot, A.N., Libourel, G., Chaussidon, M. 2004b. Oxygen isotopic compositions of the Al-rich chondrules in the CR carbonaceous chondrites: evidence for a genetic link to Ca,Al-rich inclusions and for oxygen isotope exchange during chondrule melting (abstract). *Lunar Planet. Sci.* **35**, p. 1389.

Krot, A.N., Fagan, T.J., Keil, K., McKeegan, K.D., Sahijpal, S., Hutcheon, I.D., Petaev, M.I., Yurimoto, H., 2004c. Ca, Al-rich inclusions, amoeboid olivine aggregates, and Al-rich chondrules from the unique carbonaceous chondrite Acfer 094: I. Mineralogy and petrology. *Geochim. Cosmochim. Acta* **68**, 2167–2184.

Krot, A.N., Libourel, G., Goodrich, C.A., Petaev, M.I., 2004d. Silica-rich igneous rims around magnesian chondrules in CR carbonaceous chondrites: evidence for fractional condensation during chondrule formation. *Meteorit. Planet. Sci.* **39**, 1931–1955.

Krot, A.N., Petaev, M.I., Russell, S.S., Itoh, S., Fagan, T., Yurimoto, H., Chizmadia, L., Weisberg, M.K., Komatsu, M., Ulyanov, A.A., Keil, K., 2004e. Amoeboid olivine aggregates in carbonaceous chondrites: records of nebular and asteroidal processes. *Chem. Erde* **64**, 185–239.

Krot, A.N., McKeegan, K.D., Huss, G.R., Liffman, K., Sahijpal, S., Hutcheon, I.D., Srinivasan, G., Bishoff, A., Keil, K., 2005a. Aluminum-magnesium and oxygen isotope study of relict Ca–Al-rich inclusions in chondrules. *Astrophys. J.* (in press).

Krot, A.N., Yurimoto, H., Hutcheon, I.D., MacPherson, G.J., 2005b. Relative chronology of CAI and chondrule formation: evidence from chondrule-bearing igneous CAIs. *Nature* **434**, 998–1001.

Leshin, L.A., McKeegan, K.D., Engr, C., Zanda, B., Bourot-Denise, M., Herins, R.H., 1998. Oxygen-isotopic studies of isolated and chondrule olivine from Renazzo and Allende (abstract). *Meteorit. Planet. Sci.* **33**, A93–A94.

Leshin, L.A., McKeegan, K.D., Benedix, G.K., 2000. Oxygen isotope geochemistry of olivine from carbonaceous chondrites (abstract). *Lunar Planet. Sci.* **31**, p. 1918.

Lyons, J.R., Young, E.D., 2005. CO self-shielding as the origin of oxygen isotope anomalies in the early solar nebula. *Nature* **435**, 317–320.

Maruyama, S., Yurimoto, H., Sueno, S., 1999. Oxygen isotope evidence regarding the formation of spinel-bearing chondrules. *Earth Planet. Sci. Lett.* **169**, 165–171.

Maruyama, S., Yurimoto, H., 2003. Relationship among O, Mg isotopes and the petrography of two spinel-bearing chondrules. *Geochim. Cosmochim. Acta* **67**, 3943–3957.

McKeegan, K.D., Leshin, L.A., Russell, S.S., MacPherson, G.J., 1998. Oxygen isotopic abundances in calcium–aluminum-rich inclusions from ordinary chondrites: implications for nebular heterogeneity. *Science* **280**, 414–417.

Russell, S.S., MacPherson, G.J., Leshin, L.A., McKeegan, K.D., 2000. ^{16}O enrichments in aluminum-rich chondrules from ordinary chondrites. *Earth Planet. Sci. Lett.* **184**, 57–74.

Russell, S.S., Krot, A.N., Huss, G.R., Keil, K., Itoh, S., Yurimoto, H., MacPherson, G.J., 2005. The genetic relationship between refractory inclusions and chondrules. In: Krot, A.N., Scott, E.R.D., Reipurth, B. (Eds.), *Chondrites and the Protoplanetary Disk*, vol. 341, Astronomical Society of the Pacific Conference Series, pp. 317–353.

Ryerson, F.J., McKeegan, K.D., 1994. Determination of oxygen self-diffusion in åkermanite, anorthite, diopside, and spinel: implications for oxygen isotopic anomalies and the thermal histories of Ca–Al-rich inclusions. *Geochim. Cosmochim. Acta* **58**, 3713–3734.

Scott, E.R.D., Krot, A.N., 2001. Oxygen isotopic compositions and origins of Ca–Al-rich inclusions and chondrules. *Meteorit. Planet. Sci.* **36**, 1307–1319.

Scott, E.R.D., Krot, A.N., 2003. Chondrites and their components. In: Davis, A.M. (Ed.), *Meteorites, Comets and Planets*. In: Holland, H.D., Turekian, K.K. (Eds.), *Treatise on Geochemistry*, vol. 1, Elsevier, Oxford, pp. 143–200.

Sheng, Y.J., Hutcheon, I.D., Wasserburg, G.J., 1991. Origin of plagioclase–olivine inclusions in carbonaceous chondrites. *Geochim. Cosmochim. Acta* **55**, 581–599.

Varley, L.R., Leshin, L.A., Zanda, B., Bourot-Denise, M., 2002. Correlation of oxygen isotopic composition of Renazzo olivine with degree of chondrule melting (abstract). *Meteorit. Planet. Sci.* **37**, A143.

Young, E.D., Russell, S.S., 1998. Oxygen reservoirs in the early solar nebula inferred from an Allende CAI. *Science* **282**, 452–455.

Yu, Y., Hewins, R.H., Clayton, R.N., Mayeda, T.K., 1995. Experimental study of high temperature oxygen isotope exchange during chondrule formation. *Geochim. Cosmochim. Acta* **59**, 2095–2104.

Yurimoto, H., Morioka, M., Nagasawa, H., 1989. Diffusion in single-crystals of melilite: I Oxygen. *Geochim. Cosmochim. Acta* **53**, 2387–2394.

Yurimoto, H., Nagasawa, H., Mori, Y., Matsubaya, O., 1994. Microdistribution of oxygen isotopes in a refractory inclusion from the Allende meteorite. *Earth Planet. Sci. Lett.* **128**, 47–53.

Yurimoto, H., Wasson, J.T., 2002. Extremely rapid cooling of a carbonaceous chondrite chondrule containing very ^{16}O-rich olivine and a ^{26}Mg excess. *Geochim. Cosmochim. Acta* **66**, 4355–4363.

Yurimoto, H., Kuramoto, K., 2004. Molecular cloud origin for the oxygen isotope heterogeneity in the solar system. *Science* **305**, 1763–1766.

Yurimoto, H., Ito, M., Nagasawa, H., 1998. Oxygen isotope exchange between refractory inclusion in Allende and solar nebula gas. *Science* **282**, 1874–1877.